Available online at www.sciencedirect.com
ScienceDirect
Intermetallics 16 (2008) 34–41
Intermetallics
www.elsevier.com/locate/intermet

Sliding tribological characteristics of Zr-based bulk metallic glass

Zeynep Parlar [a], Mustafa Bakkal [a,*], Albert J. Shih [b]

[a] Department of Mechanical Engineering, Istanbul Technical University, Istanbul, Turkey
[b] Department of Mechanical Engineering, University of Michigan, Ann Arbor, Michigan 48109, USA

Received 11 January 2007; accepted 13 July 2007
Available online 14 September 2007

Abstract

Wear and friction characteristics of Zr-based bulk metallic glass under dry sliding conditions are investigated. This study demonstrates that load and sliding speed significantly affect the wear characteristics of bulk metallic glass material and sliding distance is less effective on wear. Critical sliding speed and normal force limits, 1 m/s and 10 N, respectively, are distinguished. Overall average coefficient of friction value was in the range of 0.35–0.45, better than that of conventional structural materials such as AISI 6061-T6 and AISI 304. Analysis of the worn surface revealed that the bulk metallic glass was exposed to inhomogeneous shear deformation, adhesive wear, and abrasive wear during sliding test. Three sizes of wear debris, oversize flakes, machining chips and powder-like debris, are collected. There was no change recorded in surface and cross-sectional hardness measurements after the sliding test. This study concludes that bulk metallic glass is better in general friction characteristics than conventional structural materials such as AISI 6061-T6 and AISI 304.

Keywords: B. Glasses, metallic; B. Tribological properties; B. Surface properties; G. Wear-resistant applications

1. Introduction

Special metallic alloy metals under a high cooling rate can form a glassy structure. In the late 1990s, several metallic glasses with low critical cooling rates, for example $Zr_{52,5}Ti_5Cu_{17,9}Ni_{14,6}Al_{10}$ [1] and Zr41.2Ti13.8Cu12.5Ni10Be22.5 [2], were discovered. These alloys could easily be fabricated into bulk amorphous samples by cooling during casting. The discovery also made it possible to perform the fundamental tribology [3–7] studies on the bulk metallic glasses. The bulk metallic glass investigated in this study is $Zr_{52.5}Ti_5Cu_{17.9}Ni_{14.6}Al_{10}$ [1], hereafter denoted as BMG.

Distinctive mechanical, physical, and chemical properties make BMG a potential engineering material in a wide variety of applications. For example, As shown in Table 1, BMG possesses a high ultimate tensile stress (1900 MPa), high elastic strain limit (2%), low thermal conductivity (4 W/m K) and high hardness (534 kg/mm^2) compared to other conventional crystalline metals and alloys [8–10]. These properties indicated that metallic glasses could be better than conventional metals in applications.

Excellent mechanical properties of metallic glasses are a sign of promising tribological properties. Several investigations on the frictional and wear behaviors of BMGs indicated contradictory performances. Blau [3] showed no transformation evidence on worn surface. On the contrary, Fu et al. [4] reported that not only crystallization occurred on amorphous metallic glass during tribological contact but also crystalline metallic glasses are re-amorphized. Friction coefficients ranging from 0.1 and 0.9 were reported and wear resistance was either higher or equivalent to those of conventional engineering materials [2–6]. Some characteristics were common among different wear studies. For example, observations of similar plastic deformation patterns with ductile material on surface grooves [6,7] and the increase of wear rate with increasing normal load [4,7].

* Corresponding author. Tel.: +90 505 4798937; fax: +90 212 2450795.
E-mail address: bakkalmu@itu.edu.tr (M. Bakkal).

0966-9795/$ - see front matter © 2007 Elsevier Ltd. All rights reserved.
doi:10.1016/j.intermet.2007.07.011

Table 1
Properties of work and counter surface materials

Material	Elastic modulus (GPa)	Poisson ratio	Strain hardening exponent	Ultimate tensile stress (MPa)	Percent of elongation to fracture	Thermal conductivity (W/m K)	Vickers hardness (kg/mm^2)	Fracture toughness ($MPa.m^{1/2}$)
$Zr_{41.2}Ti_{13.8}Cu_{12.5}Ni_{10.0}Be_{22.5}$ BMG	*96*	*0.36*	*~0*	*1900*	*2 (all elastic)*	*4*	*534*	*40–55*
Aluminum 6061-T6	69	0.33	0.23	310	12	167	218	29
Stainless steel AISI 304	193	0.29	0.60	515	40	16.2	200	75–100
AISI 8660 (counter surface)	205	0.29	0.10	1800	5	46.6	677	75–100

The goal of this research is to study the effect of load, sliding speed, and sliding distance on wear and friction characteristics of BMG under dry condition. Results are compared with two commonly used engineering materials, aluminum 6061-T6 and AISI 304 stainless steel, denoted hereafter as Al6061 and SS304, respectively. These three work-materials have distinctly different mechanical and thermal properties, as summarized in Table 1. The experimental setup is first introduced. The effect of normal load and sliding speed on the friction coefficient is then presented. Coefficient of friction with respect to sliding distance is analyzed. Finally, wear results, SEM-EDS analysis of worn surfaces and hardness change on cross-section of worn surface, are presented to extract the distinctive wear characteristics of BMG.

2. Experimental setup

2.1. Sliding test setup

A block-on-ring apparatus was used to determine the friction and wear properties of BMG, SS304, and Al6061 on AISI 8660 ring. Configuration of the experimental setup and a picture of the BMG disc clamping and contact point of the counter surface is shown in Fig. 1. A normal load (created via dead weights) act to press the stationary test specimen onto the rotating ring. The frictional force exerted on the test specimen during sliding was measured by a force transducer placed on the pin holder. The force transducer has a load range of ±200 N with a sensitivity of ±2 mV, which is equivalent to ±0.1 N maximum measurement error. The counter surface was driven by a DC motor rotating at 30–800 rpm to achieve 0.10–2.50 m/s sliding speed. A laser infrared non-contact thermometer was used to measure the temperatures on the ring surface during testing. The wear was quantified by the loss of mass measured using a scale with ±0.0001 g accuracy. The hardness of the polished surface was measured with a Shimadzu HMV model micro-hardness tester.

2.2. Materials

A 6.35-mm diameter BMG rod was prepared at the Oak Ridge National Laboratory by a rapid casting technique [4]. The X-ray diffraction pattern for the as received BMG material is shown in Fig. 2. The ring at 38° confirms that an amorphous structure has been retained after the rapid quenching.

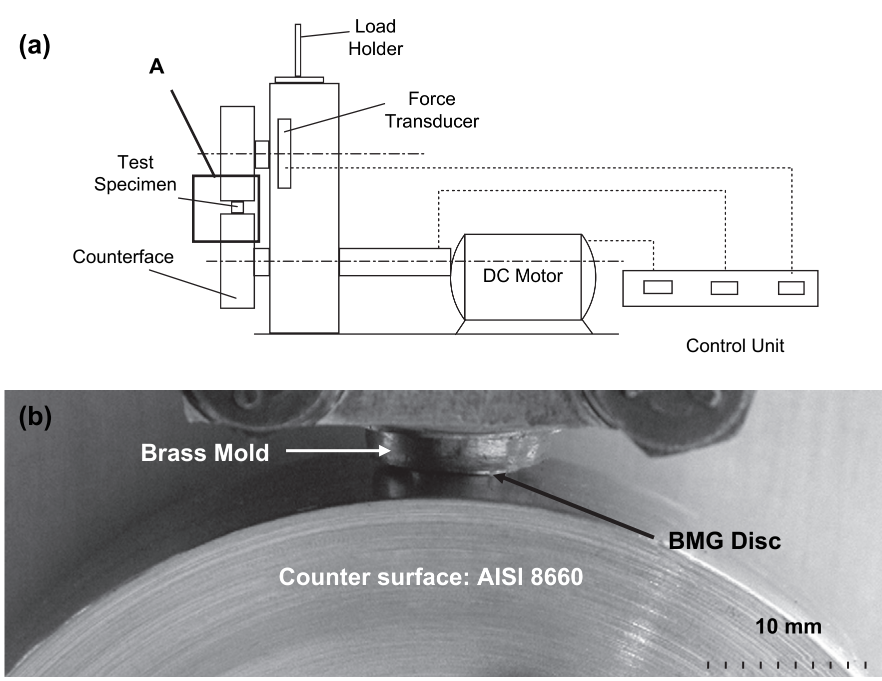

Fig. 1. (a) Configuration of the block-on-ring test setup and (b) picture of the close-up view of the box A in (a).

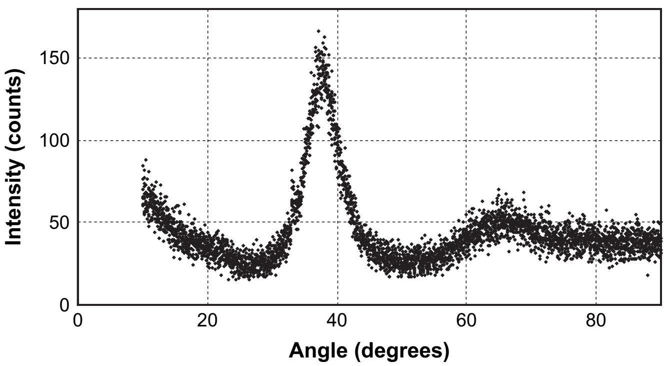

Fig. 2. X-ray intensity vs. diffraction angle (Cu Kα radiation).

The counter surface material was an AISI 8660 water quenched to HV 677 hardness. The surface roughness of the counter surface was 0.55 μm R_a. The counter face cylinder has a height of 15 mm and a diameter of 60 mm. Contact surfaces of the test specimen were machined to the same radius of curvature as the counter surface cylinder.

2.3. Test procedure

The experiments were carried out in 18–20 °C environment and 40–50% relative humidity. Before each test, both counter surface and test specimen surfaces were cleaned with carbon tetrachloride to eliminate the detrimental effect of residual debris from earlier experiments.

Three sets of test at eight different sliding speeds between 0.15 and 2.30 m/s and eight different normal loads from 5 to 40 N (in 5 N increments) were conducted to study the coefficient of friction and wear rate for BMG, Al6061, and SS304. The sliding distance was set at 100 m.

To study the effect of sliding distance on the coefficient of friction on BMG, tests were conducted at three levels of load (10, 20, and 30 N) and 10 different sliding distances from 10 to 100 m (in 10 m increments). A constant sliding speed was chosen as 0.5 m/s. The changes in the ring surface temperature and friction force with respect to the sliding distance were also recorded.

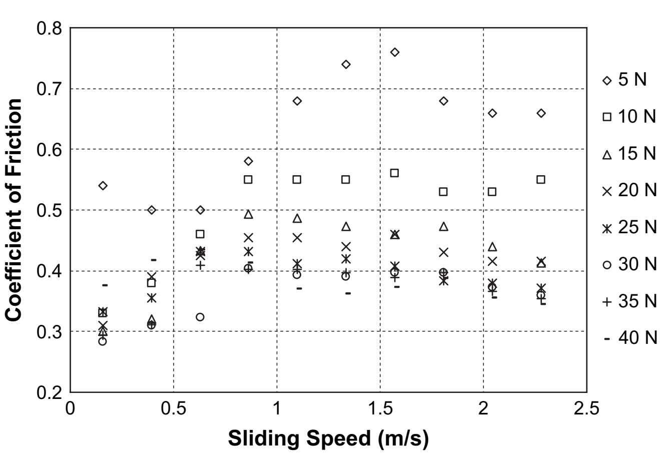

Fig. 3. The coefficient of friction μ vs. sliding speed ν for BMG.

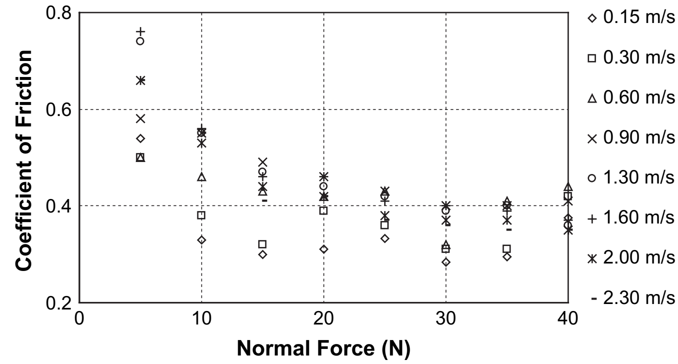

Fig. 4. BMG coefficient of friction as a function of normal loads and sliding speeds.

3. Results and discussions

3.1. Sliding tests

The coefficient of friction (μ) vs. sliding speed (ν) for BMG is shown in Fig. 3. The values for μ show a slight increase up to a speed of 1 m/s and the remainder of the data show almost no change except under the 5 N loading condition. In other words, the μ of BMG does not change significantly with the increase of sliding speed over 1 m/s given a load above 5 N. For tests over 15 N load, the μ starts from 0.3 at 0.15 m/s and then slightly increases up to 0.45 at 0.90 m/s, and, at the

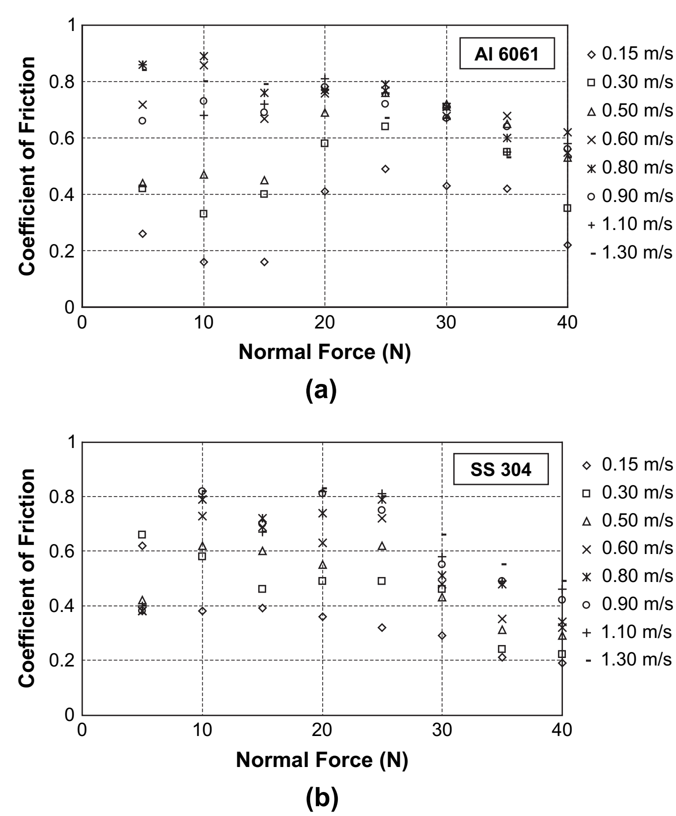

Fig. 5. The μ for (a) Al6061 and (b) SS304 as a function of normal loads and sliding speeds.

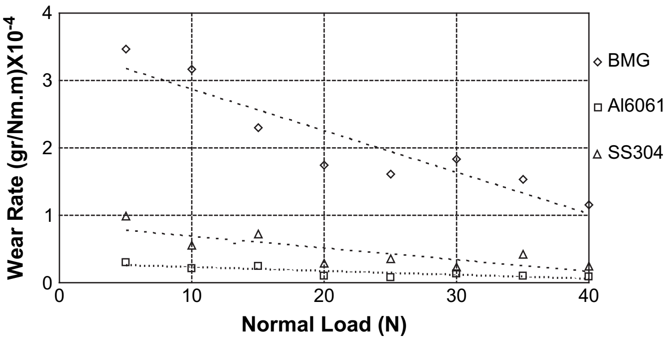

Fig. 6. Wear rate vs. normal load for BMG, Al6061 and SS304 (0.5 m/s sliding speed).

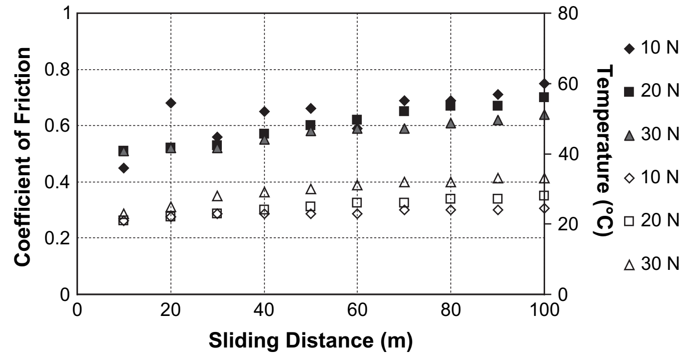

Fig. 7. BMG coefficient of friction (solid symbols) and temperature (open symbols) as a function of sliding distance (0.5 m/s sliding speed), solid marks representing the coefficient of friction.

end of the initial portion of the test, μ becomes steadier with values varying between 0.35 and 0.45. These results have an excellent agreement with the μ measured by Fluery et al. [6] under almost identical test conditions. Same loads and sliding conditions were applied to the Al6061 and SS304 materials, and the average μ was 0.7 and 0.6 for Al6061 and SS304, respectively. This result suggests that BMG has a lower μ than that of Al6061 and SS304.

For BMG, the μ at 5 N load is different. It is higher than the other loading conditions and varies greatly with respect to sliding speed. The μ was about 0.55 at the lowest speed (0.15 m/s), reduced to 0.5 at 0.6 m/s, increased to a maximum of 0.78 at 1.9 m/s, and reduced back to 0.66 at 2.3 m/s. Blau [3] reported a μ value of 0.74 at 0.25 m/s for 4.95 N normal load, which closely correlates to our test results.

Fig. 4 plots μ as a function of normal load and ν for BMG. The trend shown in Fig. 4 reflects the known trend for brittle metal-on-metal sliding contact [11]. The μ of brittle metals, first rises due to initial damage on major surface asperities at lower loads, and then decreases due to the compacted and flattened debris at higher loading conditions [11]. A sharp drop in μ was observed when changing from 5 to 10 N normal load. The reduction of μ becomes less distinct as normal loads increase. This is an indication of the consistency in sliding condition for both surfaces. The lowest μ, about 0.3, was recorded at the slowest sliding speed (0.15 m/s). Overall, the μ for BMG was in the range of 0.35–0.45. There was no distinct change in μ at higher sliding speeds.

Same testing conditions were applied to the Al6061 and SS304 materials and the results, as shown in Fig. 5(a) and (b), were different than the BMG results. The μ for Al6061 scatters below 20 N normal load. Above 20 N normal loads, a trend of reducing μ with increasing normal loads was observed. Sliding speed also affects μ. Increased sliding speed caused higher μ for Al6061. Overall, the μ for Al6061 was in the range of 0.35–0.75. For SS304, at normal loads below 20 N, the μ was also scattered. Above 20 N normal load, similar trend of μ like Al6061 was recorded. The μ was reduced with the increase of normal load. The μ for SS304 was in the range of 0.25–0.75, generally higher than that of BMG.

The wear rate of BMG vs. normal load is shown in Fig. 6. Constant sliding speed was chosen as 0.5 m/s. In general, the wear rate is reduced at higher normal load, similar to that of

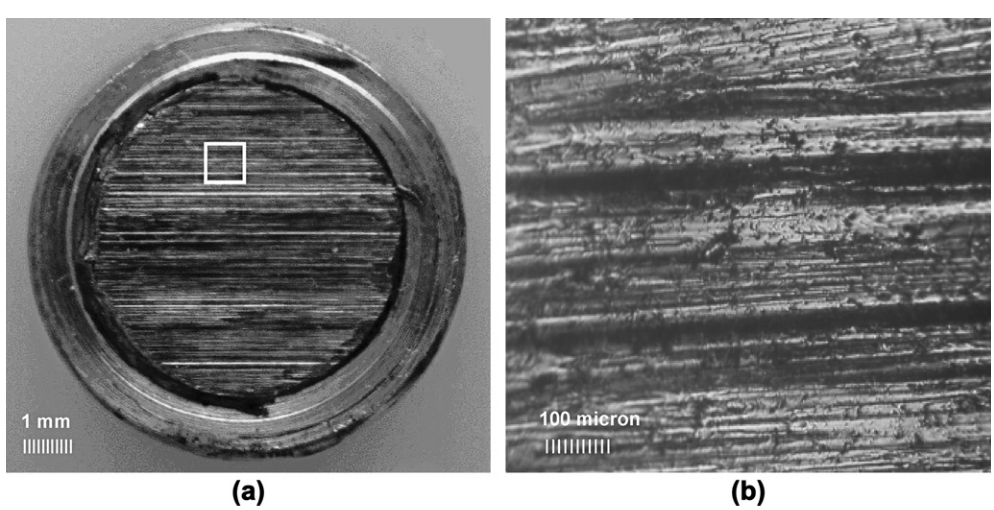

Fig. 8. Optical photomicrograph of a wear track after sliding test (40 N normal load and 1.3 m/s sliding speed): (a) overall view of worn surface and (b) detailed view of the box in (a) with the small debris of counter surface wear tracks brittle fracture surface.

the μ. After 10 N normal load there is a sharp drop in wear rate. Then, wear rate keeps on diminishing except for the slight increase at 30 N loading conditions. This result contradicts with Fu et al. [4], who reported that the wear rate increases with increasing normal load. The BMG with similar composition was tested at lower loads, max. 100 N and 10 times lower sliding speeds, 0.05 m/s. The effect of lower force and sliding speed is likely the reason of this contradiction.

During sliding, the wear rate decrease is controlled by the material transfer phenomenon between the counter surface material and the formation of protective oxide layers on the BMG surface [12]. Wear rate data for Al6061 and SS304 are also presented in Fig. 6. The hardest material, BMG, has the highest wear rate, contrary to what might be expected [7]. High wear rate of BMG is explained by their poor ductility in tension by Prakash [13]. Because the material experiences a high tensile stress during abrasive wear processes. As expected, the lowest hardness material Al6061 has better wear rate than that of SS304 due to the rule of identical metal couple [14]. The SS304 and the counterface material, AISI 8660, are steels and have poor wear performance. Diminishing wear characteristic with increasing normal load is valid for all three materials; however, effect of the increasing normal load on Al6061 and SS304 is not as distinct as BMG under the same test conditions. Due to the more distinct material transfer, Al6061 has the lowest wear rate.

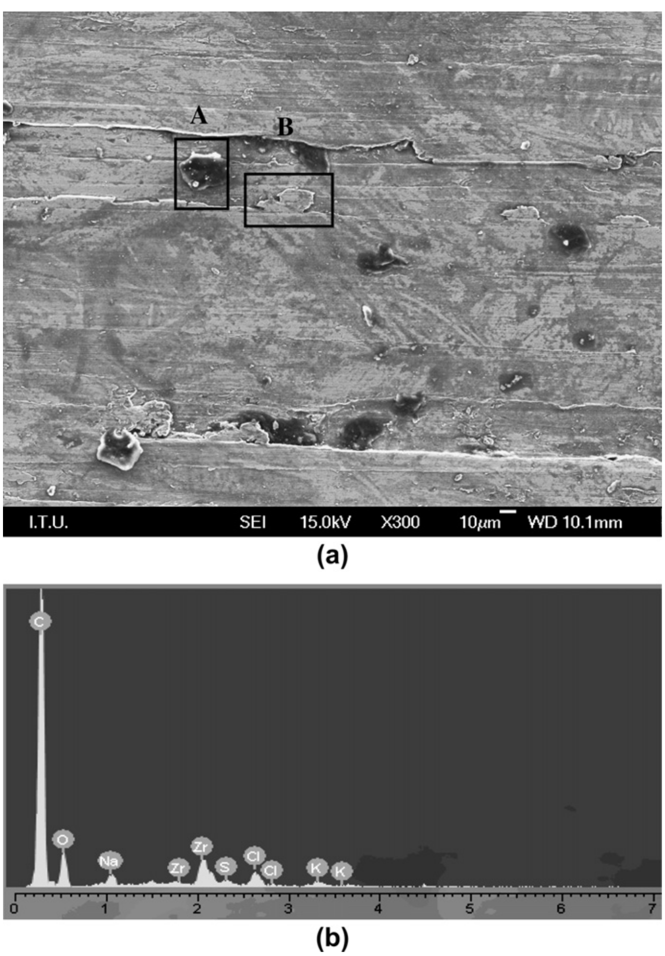

Fig. 9. SEM micrographs of the worn surface of BMG (40 N normal load and 1.3 m/s sliding speed): (a) the worn surface with grooves and black residues and (b) EDS results in counts vs. energy of the black residue indicated by box A.

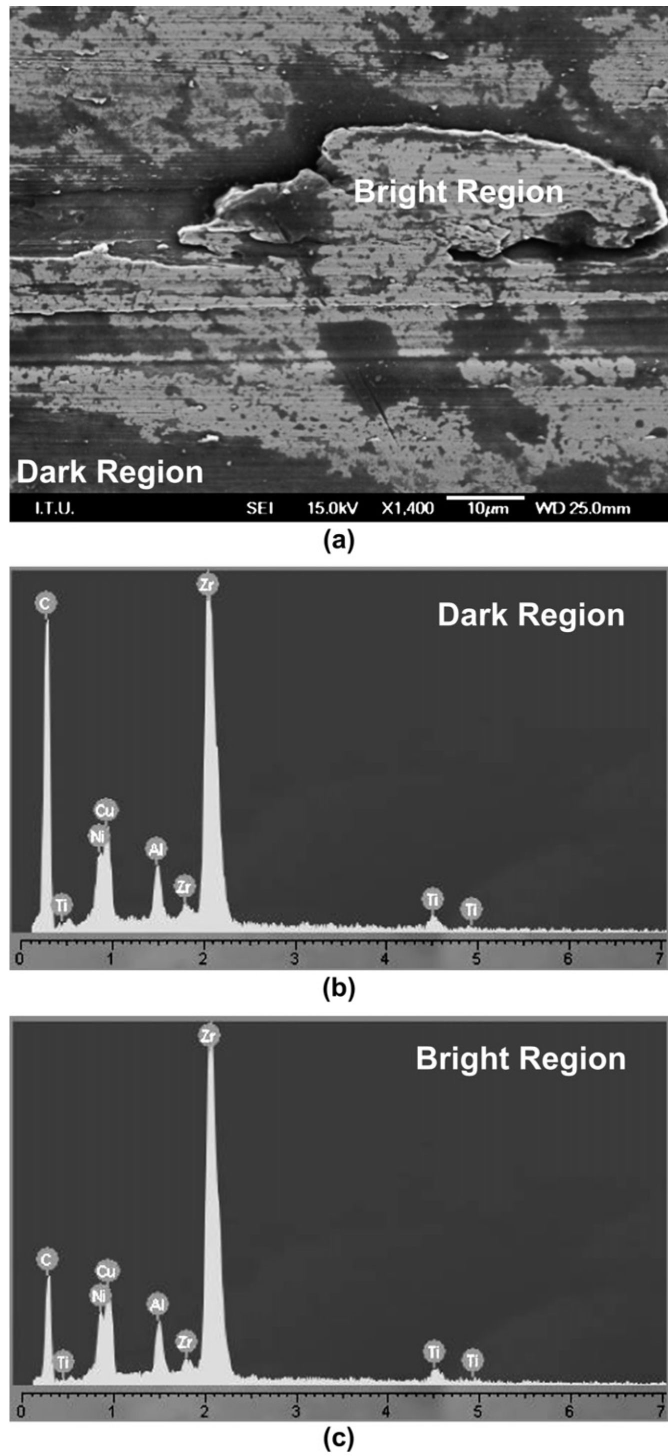

Fig. 10. SEM micrographs and EDS analysis of worn surface regions: (a) close-up view of the box B in Fig. 9(a) and identification of the dark and bright regions, and EDS result of (b) dark and (c) bright regions.

In the 20–30 N load range, two conventional structural materials, Al6061 and SS304, have the lowest wear rate and BMG has a clear drop in the wear rate. This result can be explained by counter surface characteristics. Wear force induced carbon residues and formed oxides may help to protect testing surfaces more effectively in this load range.

The friction coefficient of BMG vs. sliding distance is shown by solid symbols in Fig. 7 for three loading conditions, 10, 20 and 30 N. Temperature rise during sliding on the contact region is recorded by an infrared measurement technique and results are also presented in Fig. 7 with open symbols. At the beginning of the friction test, the coefficient of friction was about 0.5 for all normal forces. The average coefficient of friction value is about 0.6 for all force conditions. Higher normal load condition, 30 N, creates lower coefficient of friction, which is likely caused by higher sliding temperature. Similar tests were carried out for SS304 and Al6061. The average coefficient of friction values for SS304 an Al6061 are 0.5 and 0.8, respectively, after 100 m of sliding distance.

3.2. Wear track

Fig. 8 shows optical micrographs of the wear track with grooves and material flow after sliding tests. The morphology of the track indicates that the material experienced severe plastic deformation in the wear direction. Adhered material residues' transfer from counter surface can be seen in-between the grooves and on the surface (Fig. 8(b)). SEM images of these black residues are shown in Fig. 9(a). The result of EDS (Fig. 9(b)) shows that all these black residues are mainly carbon based and transferred from the steel counter surface. The presence of some oxygen in this region suggests the oxidation on residues and BMG. Since sliding tests were conducted in atmospheric conditions, chemically active elements in the BMG, such as Zr and Ti, formed a very thin oxide layer [4].

Detailed SEM and EDS analysis results of box B in Fig. 9(a) are given in Fig. 10. Chemical analysis result shows that darker regions in Fig. 10(a) have higher carbon content that of bright region. As stated earlier, carbon was transferred from the hardened AISI 8660 counter surface. Other existing elements come from the BMG.

Typical metallic glass material fracture topography evidences have been recorded at the edge of the BMG disc after the sliding test (Fig. 11(a) and (b)). Due to the severe plastic deformation during the sliding test, the worn BMG surface has shown fine abrasion marks, tearing, and grooving at the edge of BMG disc. There are typical evidences of metallic glass fracture in Fig. 11(a), void formation, river-like vein patterns, and triple ridge points due to highly inhomogeneous shear deformation. Similar formations were also reported during machining and shear punch testing of BMG [15,16]. Transferred and developed material patches on BMG surface (designated as "C") are also observed in Fig. 11(a).

Debris collected after BMG sliding tests are in a range of sizes and shapes. Three levels of debris sizes are illustrated in Fig. 12(a) (largest), (b) and (c) (smallest). It is hard to classify those chips according to the formation characteristics. Some of the reasons of these debris formations are reported earlier [3,17] as the delamination and cutting actions create oversize flakes, the abrasion wear creates miniature machining chips type debris, and adhesive in sliding wear creates sub-μm and powder size flakes.

The average surface and cross-sectional hardness measurement results of BMG disc before sliding test were 533 HV and 526 HV, respectively. After sliding test, average surface and cross-sectional hardness measurement results were 548 HV and 532 HV, respectively. Due to the insignificant change in hardness there is no micro-structural change or sliding wear-induced crystallization [18] for BMG during sliding test on given conditions.

4. Concluding remarks

This study investigated the effect of load, sliding speed and sliding distance on tribological characteristics of Zr-based BMG under dry conditions. Various loads, sliding speeds,

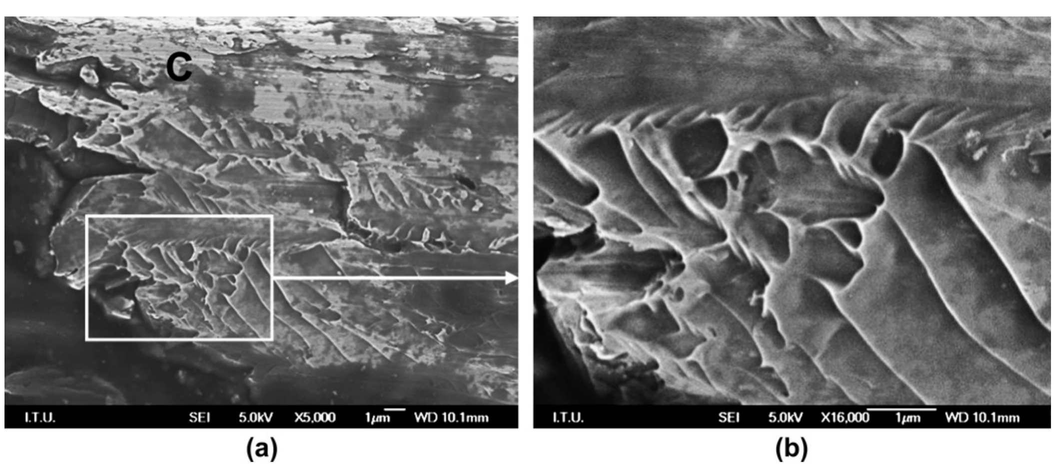

Fig. 11. SEM micrographs of the edge of BMG disc after sliding test (40 N normal load and 1.3 m/s sliding speed): (a) region C shows transferred material layer and (b) close-up view of the box in (a), showing voids, river-like vein patterns and triple ridge points of BMG fracture surface.

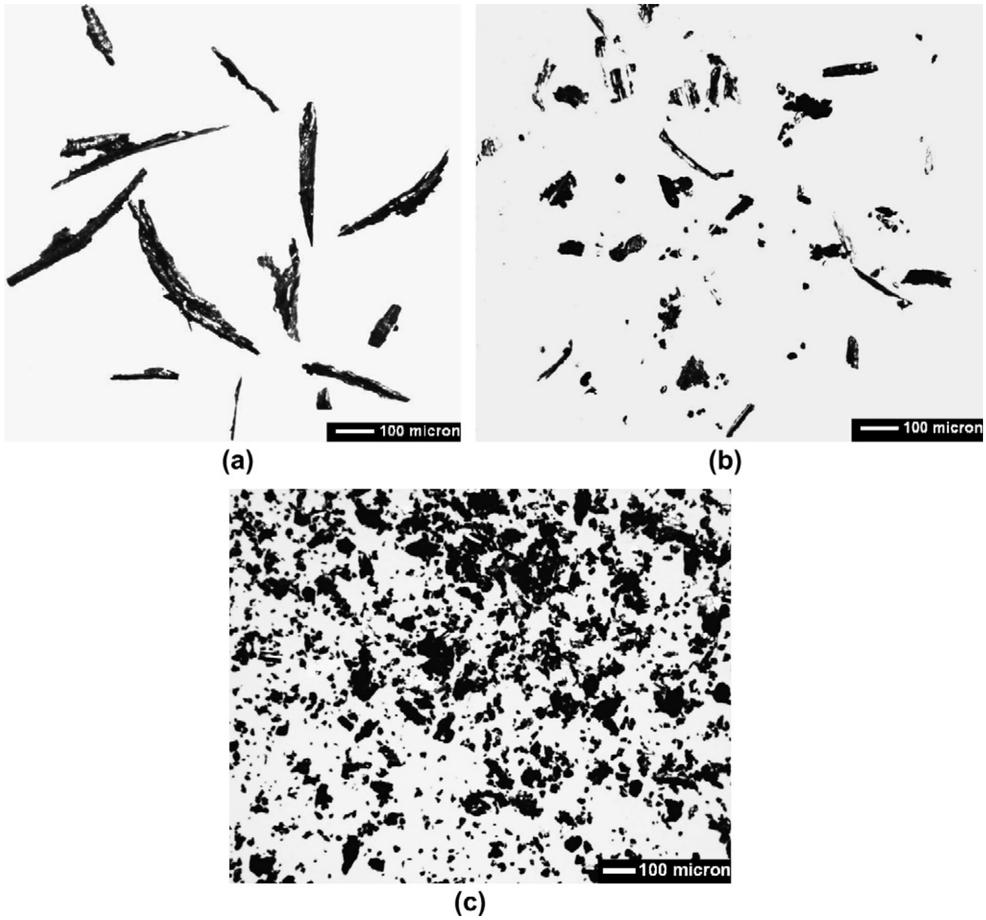

Fig. 12. Optical micrographs of wear debris (a) flakes are produced due to the cutting action and delamination between the BMG disc and counter surface, (b) machining chips are produced due to abrasion involved wear process, and (c) powder-like debris are produced due to adhesive wear action.

and sliding distances were studied. The study concluded that general friction characteristics of BMG are better than that of Al6061 and SS304 on given conditions. The μ value of BMG changes between 0.35 and 0.45 for different loading and sliding speed conditions. Only for low normal load condition (5 N) the coefficient of friction has a higher value, about 0.70. Wear rate test results showed that wear phenomenon on BMG is mainly controlled by material transfer from the counter surface. Wear track analysis of worn surface and collected wear debris have suggested that BMG surface experienced severe plastic deformation with inhomogeneous shear deformation, abrasive and adhesive wear during sliding. The sliding tests generated the surface deformations and oversize flakes, machining chips and powder-like debris collected for BMG. There was no significant change in hardness after testing. Micro-hardness test results suggested that the BMG had good thermal stability and there was no sliding induced crystallization under test conditions conducted in this study.

Acknowledgements

The authors acknowledge the BMG material provided by Dr. C. T. Liu of Oak Ridge National Lab.

References

[1] Liu CT, Heatherly L, Easton DS, Carmichael CA, Schneibel JH, Chen CH, et al. Test environments and mechanical properties of Zr-base bulk amorphous alloys. Metallurgical And Materials Transactions A 1998;29:1811–20.
[2] Peker A, Johnson WL. A highly processable metallic glass: Zr41Ti14-Cu12.5Ni10Be22.5. Applied Physics Letters 1993;63:2342–4.
[3] Blau PJ. Friction and wear of a Zr-based amorphous metal alloy under dry and lubricated conditions. Wear 2001;250:431–4.
[4] Fu X-Y, Kasai T, Falk ML, Rigney DA. Sliding behavior of metallic glass – Part I. Experimental investigations. Wear 2001;250:409–19.
[5] Klinger R, Feller HG. Sliding friction and wear resistance of the metallic glass $Fe_{40}Ni_{40}B_{20}$. Wear 1983;86(2):287–97.
[6] Fluery E, Lee SM, Ahn HS, Kim WT, Kim DH. Tribological properties of bulk metallic glasses. Materials Science and Engineering A 2004;375–377:276–9.
[7] Tam CY, Shek CH. Abrasive wear of $Cu_{60}Zr_{30}Ti_{10}$ bulk metallic glass. Materials Science and Engineering A 2004;384(1–2):138–42.
[8] Loeffler JF. Bulk metallic glasses. Intermetallics 2003;11:529–40.
[9] Bakkal M, Liu CT, Watkins T, Scattergood RO, Shih AJ. Oxidation and crystallization of Zr-based bulk metallic glass due to machining. Intermetallics 2004;12:195–204.
[10] Bakkal M, Shih AJ, Scattergood RO, Liu CT. Machining of a Zr–Ti–Al–Cu–Ni metallic glass. Scripta Materialia 2004;50:583–8.
[11] Ludema KC. Friction, wear, lubrication: a text book in tribology. Boca Raton: CRC Press; 1996.

[12] Prakash B, Hiratsuka K. Sliding wear behaviour of some Fe-, Co- and Ni-based metallic glasses during rubbing against bearing steel. Tribology Letters 2000;8(2−3):153−60.
[13] Prakash B. Abrasive behaviour of Fe, Co and Ni based metallic glasses. Wear 2005;258:217−24.
[14] Bhushan B. Introduction to tribology. New York: John Wiley and Sons; 2002.
[15] Guduru RK, Darling KA, Scattergood RO, Koch CC, Murty KL, Bakkal M, et al. Shear punch tests for a bulk metallic glass. Intermetallics 2006;14:1411−6.
[16] Bakkal M, Shih AJ, McSpadden SB, Liu CT, Scattergood RO. Light emission, chip morphology, and burr formation in drilling the bulk metallic glass. International Journal of Machine Tools Manufacture 2005;45:741−52.
[17] Davis JR. ASM specialty handbook, carbon and alloy steels. ASM International; 1995.
[18] Li G, Wang YQ, Wang LM, Gao YP, Zhang RJ, Zhan ZJ, et al. Wear behavior of bulk $Zr_{41}Ti_{14}Cu_{12.5}Ni_{10}Be_{22.5}$ metallic glasses. Journal of Materials Research 2002;17(8):1877−80.